

Extracting kinetic parameters from FRAP and FLIP experiments

Shai Carmi

June 12, 2011

1 A Reaction-Diffusion model

1.1 Preliminary assumptions

Our approach is an adaptation of the models proposed in [1] and later in [2]. We first assume our system is two dimensional, or in other words, has cylindrical symmetry. This assumption, justified in [2], requires that both the laser profile and the nucleus and its contents do not vary along the z -axis. This also means circular symmetry of the nucleus with respect to the center of the bleaching spot. Denote the tagged proteins as our ‘particles’ or ‘molecules’. We assume particles do not experience drift (directed transport) and that binding sites are evenly spread in the parts of the nucleus where they exist (compare, e.g., [3]). We also use the standard assumption that the system is in equilibrium prior to the bleaching and remains so during the entire bleaching and observation periods. Put differently, we assume bleaching only affects the visibility, but not any other chemical or physical property, of the particles. The bleaching profile is assumed to be perfectly circular, that is, all molecules within radius r_s , and only these molecules, lose their fluorescence at time $t = 0$ when the bleaching step ends. See Section 2.1 for a discussion on the validity of this assumption and on implementation issues. The nucleus is assumed to be a perfect circle of finite radius r_n .

1.2 FRAP Model definition

We assume particles diffuse freely (perform Brownian motion) and also react with a single type of binding sites (for treatment of multiple binding states see Section 1.6). The reaction is



where F represents free particles, S represents empty binding sites, and C stands for FS complexes. The reaction on- and off- rates are k_{on} and k_{off} , respectively, and are r -dependent with the following general form:

$$\begin{aligned} k_{\text{on}}(r) &= \begin{cases} k_{\text{on}}^{(i)} & r < r_s, \\ k_{\text{on}}^{(o)} & r_s < r < r_n. \end{cases} \\ k_{\text{off}}(r) &= \begin{cases} k_{\text{off}}^{(i)} & r < r_s, \\ k_{\text{off}}^{(o)} & r_s < r < r_n. \end{cases} \end{aligned} \quad (2)$$

We state below our results for any general combination of $k_{\text{on}}^{(i)}$, $k_{\text{off}}^{(i)}$, $k_{\text{on}}^{(o)}$, $k_{\text{off}}^{(o)}$. However, the specific cases that will be of highest biological interest are:

- Homogeneous binding. In that case, $k_{\text{on}}^{(i)} = k_{\text{on}}^{(o)}$ and $k_{\text{off}}^{(i)} = k_{\text{off}}^{(o)}$, namely the reaction rate is the same everywhere in the nucleus.
- Internal binding. In that case, $k_{\text{on}}^{(i)} > 0$ and $k_{\text{on}}^{(o)} = 0$, namely the reaction occurs only inside the bleached spot but not outside ($k_{\text{off}}^{(i)} > 0$, $k_{\text{off}}^{(o)}$ is irrelevant in this case).
- External binding. In that case, $k_{\text{on}}^{(i)} = 0$ and $k_{\text{on}}^{(o)} > 0$, namely the reaction occurs only outside the spot.

In addition to the free and bound particles, we assume that some particles are inert and immobile. These (fluorescent) particles, which we call the static particles, reside in the nucleus, evenly distributed, but do not move or participate in any reaction.

Denote the concentrations of the *visible* particles as $f = [F]$, $c = [C]$, and $\beta = [B]$, and the concentration of the binding sites as $s = [S]$. As in [1], we assume the concentration of the binding sites is constant throughout the experiment, or $s = s_{\text{eq}}$, because the chemical equilibrium is not disturbed by the bleaching. We further assume $[FS]$ complexes are immobile (compare, e.g., [4]). We can thus write the following set of reaction-diffusion equations:

$$\begin{aligned} \frac{\partial f(r, t)}{\partial t} &= D\nabla^2 f(r, t) - k_{\text{on}}f(r, t)s_{\text{eq}} + k_{\text{off}}c(r, t), \\ \frac{\partial c(r, t)}{\partial t} &= k_{\text{on}}f(r, t)s_{\text{eq}} - k_{\text{off}}c(r, t), \\ \beta(r, t) &= \beta(r, t = 0), \end{aligned} \quad (3)$$

where D is the diffusion coefficient of the free particles. Eq. (3) is valid for $t \geq 0$, $0 < r < r_n$. Note that $f = f(r, \theta, t) = f(r, t)$ and $c = c(r, \theta, t) =$

$c(r, t)$ due to the assumed circular symmetry. The concentration of the free particles, f , and its derivative must be continuous at $r = r_s$. However the concentration of the bound particles need not be. The static particles do not move and do not participate in the reaction and therefore the equation for their evolution is trivial and will be usually omitted henceforth.

To simplify the Eq. (3), let $k_{\text{on}}^* = k_{\text{on}} s_{\text{eq}}$ be the pseudo-on rate,

$$\begin{aligned}\frac{\partial f}{\partial t} &= D\nabla^2 f - k_{\text{on}}^* f + k_{\text{off}} c, \\ \frac{\partial c}{\partial t} &= k_{\text{on}}^* f - k_{\text{off}} c.\end{aligned}\tag{4}$$

To simplify the notation, in the following we denote the pseudo-on rate simply as the ‘on rate’ and k_{on}^* just as k_{on} . Our equations can thus be finally written as

$$\begin{aligned}\frac{\partial f}{\partial t} &= D\nabla^2 f - k_{\text{on}} f + k_{\text{off}} c, \\ \frac{\partial c}{\partial t} &= k_{\text{on}} f - k_{\text{off}} c.\end{aligned}\tag{5}$$

The boundary condition is:

$$\left. \frac{\partial}{\partial r} f(r, t) \right|_{r=r_n} = 0,\tag{6}$$

namely the boundaries of the nucleus serve as reflecting walls [5].

In FRAP, bleaching at $t = 0$ removes all visible molecules from the bleaching spot $r < r_s$. Thus, the initial conditions are given as follows. For the static particles,

$$\beta(r, t = 0) = \begin{cases} 0 & r < r_s, \\ \beta & r_s < r < r_n, \end{cases}\tag{7}$$

because before the bleach, the concentration of the static particles is constant in space and can be simply denoted with β . For f and c ,

$$\begin{aligned}f(r, t = 0) &= \begin{cases} 0 & r < r_s, \\ f_{\text{eq}}^{(o)} & r_s < r < r_n. \end{cases} \\ c(r, t = 0) &= \begin{cases} 0 & r < r_s, \\ c_{\text{eq}}^{(o)} & r_s < r < r_n, \end{cases}\end{aligned}\tag{8}$$

where $f_{\text{eq}}^{(o)}$ and $c_{\text{eq}}^{(o)}$ are the equilibrium concentrations of f and c , respectively, for $r_s < r < r_n$. To find these, we calculate first the equilibrium concentrations for $r < r_s$, $f_{\text{eq}}^{(i)}$ and $c_{\text{eq}}^{(i)}$. In equilibrium, all time derivatives vanish. Thus $k_{\text{on}}^{(i)} f_{\text{eq}}^{(i)} - k_{\text{off}}^{(i)} c_{\text{eq}}^{(i)} = 0$. This gives one equation for $f_{\text{eq}}^{(i)}$ and $c_{\text{eq}}^{(i)}$. To find another equation, we need to define the detected signal.

Let the macroscopic measured signal in a FRAP experiment be the average concentration of visible molecules across the circle $r < r_m$,

$$\mathcal{I}(t) = \frac{1}{\pi r_m^2} \int_0^{r_m} 2\pi r [f(r, t) + c(r, t) + \beta(r, t)] dr. \quad (9)$$

We denote $r_m \leq r_s$ as the monitoring radius. $\mathcal{I}(t)$ will later be calculated analytically and compared to the experimental signal. At $t = 0$, we demand normalization or that $\mathcal{I}(t) = 1$ (Section 2.4). Since in equilibrium $f(r < r_s) = f_{\text{eq}}^{(i)}$ and $c(r < r_s) = c_{\text{eq}}^{(i)}$, we have by normalization at $t = 0$ that $f_{\text{eq}}^{(i)} + c_{\text{eq}}^{(i)} + \beta = 1$. This is our second equation for $f_{\text{eq}}^{(i)}$ and $c_{\text{eq}}^{(i)}$ from which we have $f_{\text{eq}}^{(i)} = (1 - \beta) \frac{k_{\text{off}}^{(i)}}{k_{\text{on}}^{(i)} + k_{\text{off}}^{(i)}}$ and $c_{\text{eq}}^{(i)} = (1 - \beta) \frac{k_{\text{on}}^{(i)}}{k_{\text{on}}^{(i)} + k_{\text{off}}^{(i)}}$. Since f must be continuous, we have $f_{\text{eq}}^{(o)} = f_{\text{eq}}^{(i)}$. The time derivatives vanish also for $r_s < r < r_n$, and hence $c_{\text{eq}}^{(o)} = \frac{k_{\text{on}}^{(o)}}{k_{\text{off}}^{(o)}} f_{\text{eq}}^{(o)}$. Thus, we finally reach

$$\begin{aligned} f_{\text{eq}}^{(o)} &= (1 - \beta) \frac{k_{\text{off}}^{(i)}}{k_{\text{on}}^{(i)} + k_{\text{off}}^{(i)}}, \\ c_{\text{eq}}^{(o)} &= (1 - \beta) \frac{k_{\text{on}}^{(o)}}{k_{\text{off}}^{(o)}} \frac{k_{\text{off}}^{(i)}}{k_{\text{on}}^{(i)} + k_{\text{off}}^{(i)}}, \end{aligned} \quad (10)$$

and by that we specified the initial conditions.

Eq. (10) for the equilibrium concentrations, along with Eqs. (2), (5), (6), and (8) for the differential equations system, and with Eq. (9) for the detected signal, completely define the model.

1.3 Computational framework

The computational approach can be outlined as follows:

1. Set the parameters r_m , r_s , r_n , β , and the binding model (homogeneous/internal/external binding) according to the experimental setup.
2. Given D , k_{on} , and k_{off} , solve the system of equations (5), (6), and (8), and obtain $\mathcal{I}(t)$.

3. Compare $\mathcal{I}(t)$ calculated from the model to the experimentally measured intensity $\mathcal{I}_{\text{exp}}(t)$. Record the difference.
4. Modify D , k_{on} , and k_{off} , and jump to step 2.
5. Report the values of D , k_{on} , and k_{off} that gave the best fit to the experimental data.

Note that although in principle there are four reaction rate parameters $k_{\text{on}}^{(i)}$, $k_{\text{off}}^{(i)}$, $k_{\text{on}}^{(o)}$, $k_{\text{off}}^{(o)}$, in the practical cases of interest (homogeneous/internal/external binding) there are only two free parameters and the other pair of parameters are either zero/irrelevant or are determined from the first two (Section 1.2). We can therefore refer unambiguously to the reaction rate parameters as just k_{on} and k_{off} . Details on the implementation of the various steps, and in particular, on the search in the parameter space to find the best fit, are given in Section 2.6.

1.4 FRAP Model solution

To solve Eq. (5) and find the total intensity $\mathcal{I}(t)$, we Laplace transform Eq. (5) $t \rightarrow p$. Using the Laplace identity $\mathcal{L}\left\{\frac{\partial f}{\partial t}\right\} = pf - f(t=0)$, this yields for $r < r_s$

$$\begin{aligned} pf(r, p) &= D\nabla^2 f(r, p) - k_{\text{on}}^{(i)} f(r, p) + k_{\text{off}}^{(i)} c(r, p), \\ pc(r, p) &= k_{\text{on}}^{(i)} f(r, p) - k_{\text{off}}^{(i)} c(r, p). \end{aligned} \quad (11)$$

For $r_s < r < r_n$,

$$\begin{aligned} pf(r, p) - f_{\text{eq}}^{(o)} &= D\nabla^2 f(r, p) - k_{\text{on}}^{(o)} f(r, p) + k_{\text{off}}^{(o)} c(r, p), \\ pc(r, p) - c_{\text{eq}}^{(o)} &= k_{\text{on}}^{(o)} f(r, p) - k_{\text{off}}^{(o)} c(r, p). \end{aligned} \quad (12)$$

We use along this document the convention that the variable in parenthesis defines the space we are working in. Thus, $f(r, p)$ is the Laplace transform $t \rightarrow p$ of $f(r, t)$, etc. (we occasionally even omit the arguments when they are clear from the context). The equation for c is algebraic and is easily solved in terms of f ,

$$c(r, p) = \begin{cases} \frac{k_{\text{on}}^{(i)} f(r, p)}{p + k_{\text{off}}^{(i)}} & r < r_s, \\ \frac{c_{\text{eq}}^{(o)} + k_{\text{on}}^{(o)} f(r, p)}{p + k_{\text{off}}^{(o)}} & r_s < r < r_n. \end{cases} \quad (13)$$

Substituting Eq. (13) in Eq. (12) we obtain the following ordinary differential equation for f :

$$\nabla^2 f(r, p) = \begin{cases} q_i^2 f(r, p) & r < r_s, \\ q_o^2 f(r, p) - V & r_s < r < r_n, \end{cases} \quad (14)$$

where

$$\begin{aligned} q_i^2 &= \frac{p}{D} \left(1 + \frac{k_{\text{on}}^{(i)}}{p + k_{\text{off}}^{(i)}} \right), \\ q_o^2 &= \frac{p}{D} \left(1 + \frac{k_{\text{on}}^{(o)}}{p + k_{\text{off}}^{(o)}} \right), \end{aligned} \quad (15)$$

and

$$V = \frac{f_{\text{eq}}^{(o)}}{D} \left(1 + \frac{k_{\text{on}}^{(o)}}{p + k_{\text{off}}^{(o)}} \right). \quad (16)$$

In the equation for V we used the relation $c_{\text{eq}}^{(o)} = \left(k_{\text{on}}^{(o)} / k_{\text{off}}^{(o)} \right) f_{\text{eq}}^{(o)}$. Writing the Laplacian in Eq. (14) in cylindrical coordinates, we have

$$\frac{\partial^2 f}{\partial r^2} + \frac{1}{r} \frac{\partial f}{\partial r} = \begin{cases} q_i^2 f & r < r_s, \\ q_o^2 f - V & r_s < r < r_n. \end{cases} \quad (17)$$

The solution of the last equation is a combination of modified Bessel functions of the first and second kinds [6]:

$$f = \begin{cases} AI_0(q_i r) & r < r_s, \\ BI_0(q_o r) + CK_0(q_o r) + \frac{V}{q_o^2} & r_s < r < r_n, \end{cases} \quad (18)$$

where we eliminated the modified Bessel function of the second kind K_0 in the region $r < r_s$ because K_0 diverges at $r = 0$. We now demand continuity of f and its first derivative at $r = r_s$ and the boundary condition at r_n . This results in the following linear system of equations for the coefficients $\{A, B, C\}$:

$$\begin{aligned} AI_0(q_i r_s) &= BI_0(q_o r_s) + CK_0(q_o r_s) + \frac{V}{q_o^2}, \\ Aq_i I_1(q_i r_s) &= Bq_o I_1(q_o r_s) - Cq_o K_1(q_o r_s), \\ BI_1(q_o r_n) - CK_1(q_o r_n) &= 0, \end{aligned} \quad (19)$$

where we used the relations $I_0'(r) = I_1(r)$ and $K_0'(r) = -K_1(r)$. The solution of these equations is:

$$\begin{aligned} A &= \frac{V q_o}{q_o^2 q_i} \frac{I_1(q_o r_s) K_1(q_o r_n) - I_1(q_o r_n) K_1(q_o r_s)}{\text{den}}, \\ B &= \frac{V}{q_o^2} \frac{I_1(q_i r_s) K_1(q_o r_n)}{\text{den}}, \\ C &= \frac{V}{q_o^2} \frac{I_1(q_i r_s) I_1(q_o r_n)}{\text{den}}. \end{aligned} \quad (20)$$

where

$$\begin{aligned} \text{den} &= (q_i/q_o) I_0(q_i r_s) [I_1(q_o r_s) K_1(q_o r_n) - I_1(q_o r_n) K_1(q_o r_s)] \\ &\quad - I_1(q_i r_s) [I_1(q_o r_n) K_0(q_o r_s) + I_0(q_o r_s) K_1(q_o r_n)]. \end{aligned} \quad (21)$$

We thus obtained f for all r . Using f , the concentration of bound complexes c is given in Eq. (13). The total signal is (in Laplace p space)

$$\begin{aligned} \mathcal{I}(p) &= \frac{1}{\pi r_m^2} \int_0^{r_m} 2\pi r [f(r, p) + c(r, p) + \beta(r, p)] dr \\ &= \frac{1}{r_m^2} \int_0^{r_m} 2r f(r, p) \left(1 + \frac{k_{\text{on}}^{(i)}}{p + k_{\text{off}}^{(i)}} \right) dr \\ &= 2A \frac{1}{r_m^2} \left(1 + \frac{k_{\text{on}}^{(i)}}{p + k_{\text{off}}^{(i)}} \right) \int_0^{r_m} r I_0(q_i r) dr \\ &= 2A \left(1 + \frac{k_{\text{on}}^{(i)}}{p + k_{\text{off}}^{(i)}} \right) \frac{I_1(q_i r_m)}{q_i r_m}. \end{aligned} \quad (22)$$

Since $r_m < r_s$, we could use the expressions for f , c , and β in $r < r_s$ (e.g., $\beta(r < r_s, t) = 0$, etc.). To solve the integral, we used the relation $[rI_1(r)]' = rI_0(r)$. Note that A is given in Eq. (20) in terms of the given parameters r_s , and r_n , as well as in terms of V , q_i , and q_o , which are given in turn in Eqs. (15) and (16) in terms of p and β , D , $k_{\text{on}}^{(i)}$, $k_{\text{off}}^{(i)}$, $k_{\text{on}}^{(o)}$, $k_{\text{off}}^{(o)}$. Thus, we obtained the total signal in terms of p and the given parameters. To obtain $\mathcal{I}(t)$, we need only invert Eq. (22) with respect to p . This is done numerically, as explained in Section 2.6.

1.5 Limiting cases

1.5.1 Infinite time

Let the concentration of free and bound particles at $t \rightarrow \infty$ be f_∞ and c_∞ , respectively. When $t \rightarrow \infty$, all free particles are evenly distributed in the

nucleus. Thus for all $r < r_s$, $c_\infty = \frac{k_{\text{on}}^{(i)}}{k_{\text{off}}^{(i)}} f_\infty$, while for $r_s < r < r_n$, $c_\infty = \frac{k_{\text{on}}^{(o)}}{k_{\text{off}}^{(o)}} f_\infty$. Static particles exist at all times in $r_s < r < r_n$ in concentration β . Let the total number of visible particles be N , and define $\rho_i \equiv \frac{k_{\text{on}}^{(i)} + k_{\text{off}}^{(i)}}{k_{\text{off}}^{(i)}}$ and $\rho_o \equiv \frac{k_{\text{on}}^{(o)} + k_{\text{off}}^{(o)}}{k_{\text{off}}^{(o)}}$. Then:

$$\begin{aligned} N &= f_\infty \left[\pi r_s^2 \left(1 + \frac{k_{\text{on}}^{(i)}}{k_{\text{off}}^{(i)}} \right) + \pi (r_n^2 - r_s^2) \left(1 + \frac{k_{\text{on}}^{(o)}}{k_{\text{off}}^{(o)}} \right) \right] + \beta \pi (r_n^2 - r_s^2) \\ &= f_\infty \pi [r_s^2 \rho_i + (r_n^2 - r_s^2) \rho_o] + \beta \pi (r_n^2 - r_s^2). \end{aligned} \quad (23)$$

The total number of visible particles can also be computed from the initial conditions at $t = 0$:

$$\begin{aligned} N &= f_{\text{eq}}^{(o)} \pi (r_n^2 - r_s^2) \left(1 + \frac{k_{\text{on}}^{(o)}}{k_{\text{off}}^{(o)}} \right) + \beta \pi (r_n^2 - r_s^2) \\ &= (1 - \beta) \frac{k_{\text{off}}^{(i)}}{k_{\text{on}}^{(i)} + k_{\text{off}}^{(i)}} \pi (r_n^2 - r_s^2) \left(1 + \frac{k_{\text{on}}^{(o)}}{k_{\text{off}}^{(o)}} \right) + \beta \pi (r_n^2 - r_s^2) \\ &= (1 - \beta) \pi (r_n^2 - r_s^2) \frac{\rho_o}{\rho_i} + \beta \pi (r_n^2 - r_s^2). \end{aligned} \quad (24)$$

Equating the last two equations we obtain,

$$f_\infty = (1 - \beta) \frac{1}{\rho_i} \frac{(1 - \epsilon^2) \rho_o}{\epsilon^2 \rho_i + (1 - \epsilon^2) \rho_o}, \quad (25)$$

where $\epsilon = r_s/r_n < 1$. The signal for long times is

$$\begin{aligned} \mathcal{I}(t \rightarrow \infty) &= \left(1 + \frac{k_{\text{on}}^{(i)}}{k_{\text{off}}^{(i)}} \right) f_\infty = \rho_i f_\infty \\ &= (1 - \beta) \frac{1}{1 + \frac{\epsilon^2}{1 - \epsilon^2} \frac{\rho_i}{\rho_o}}. \end{aligned} \quad (26)$$

Note that $\mathcal{I}(t \rightarrow \infty) < 1$ because visible particles were removed at $t = 0$ and thus recovery cannot be complete. Also note that for $\epsilon \rightarrow 0$ (an infinite nucleus), the signal at long time is $(1 - \beta)$, which is the *mobile* fraction.

1.5.2 The reaction-dominant limit

Consider the case when diffusion is extremely fast such that $D \rightarrow \infty$. In this case, the concentration of the free particles is always the same everywhere the nucleus. The system of equations (5) becomes:

$$\begin{aligned}\frac{\partial c^{(i)}}{\partial t} &= k_{\text{on}}^{(i)} f - k_{\text{off}}^{(i)} c^{(i)}, \\ \frac{\partial c^{(o)}}{\partial t} &= k_{\text{on}}^{(o)} f - k_{\text{off}}^{(o)} c^{(o)}, \\ \frac{\partial f}{\partial t} &= \frac{1}{\pi r_n^2} \left[\pi r_s^2 \left(-\frac{\partial c^{(i)}}{\partial t} \right) + \pi (r_n^2 - r_s^2) \left(-\frac{\partial c^{(o)}}{\partial t} \right) \right] \\ &= \epsilon^2 \left(k_{\text{off}}^{(i)} c^{(i)} - k_{\text{on}}^{(i)} f \right) + (1 - \epsilon^2) \left(k_{\text{off}}^{(o)} c^{(o)} - k_{\text{on}}^{(o)} f \right),\end{aligned}\quad (27)$$

where $c^{(i)}$ and $c^{(o)}$ are the concentrations of bound particles for $r < r_s$ and $r_s < r < r_n$, respectively, and $\epsilon = r_s/r_n$ (Section 1.5.1). Note that $c^{(i)}$, $c^{(o)}$, and f are constants in space, and thus (27) is a system of ordinary differential equations. The equation for f is justified as follows. Clearly, the increase (per unit time) in the total number of free molecules is equal to the total decrease in the number of bound molecules, $\pi r_s^2 \left(-\frac{\partial c^{(i)}}{\partial t} \right) + \pi (r_n^2 - r_s^2) \left(-\frac{\partial c^{(o)}}{\partial t} \right)$. Molecules that become free are immediately evenly distributed throughout the nucleus, and thus the increase in the concentration of free molecules is obtained by dividing the last expression by the total area of the nucleus, πr_n^2 .

Let us specify the initial conditions of Eq. (27). Denote by $f_{\text{pb}} = f(t = 0)$ the post-bleaching concentration of the free particles. To calculate f_{pb} , we recall that at $t < 0$, $f = f_{\text{eq}}^{(o)} = f_{\text{eq}}^{(i)} = f_{\text{eq}} = (1 - \beta) \frac{k_{\text{off}}^{(i)}}{k_{\text{on}}^{(i)} + k_{\text{off}}^{(i)}}$ and write a conservation of material equation for the free particles $f_{\text{pb}} \pi r_n^2 = f_{\text{eq}} \pi (r_n^2 - r_s^2)$. Thus, $f_{\text{pb}} = (1 - \epsilon^2) f_{\text{eq}}$. For $r < r_s$, $c^{(i)}(t = 0) = 0$. For $r_s < r < r_n$, $c^{(o)}(t = 0) = c_{\text{eq}}^{(o)} = (1 - \beta) \frac{k_{\text{on}}^{(o)}}{k_{\text{off}}^{(o)}} \frac{k_{\text{off}}^{(i)}}{k_{\text{on}}^{(i)} + k_{\text{off}}^{(i)}}$. As in Section 1.4, we Laplace transform Eq. (27) $t \rightarrow p$. This yields:

$$\begin{aligned}pc^{(i)} &= k_{\text{on}}^{(i)} f - k_{\text{off}}^{(i)} c^{(i)}, \\ pc^{(o)} - c_{\text{eq}}^{(o)} &= k_{\text{on}}^{(o)} f - k_{\text{off}}^{(o)} c^{(o)}, \\ pf - (1 - \epsilon^2) f_{\text{eq}} &= \epsilon^2 \left(k_{\text{off}}^{(i)} c^{(i)} - k_{\text{on}}^{(i)} f \right) + (1 - \epsilon^2) \left(k_{\text{off}}^{(o)} c^{(o)} - k_{\text{on}}^{(o)} f \right).\end{aligned}\quad (28)$$

This is an algebraic system of equations. The solution of this system is

$$\begin{aligned}
c^{(i)} &= \frac{k_{\text{on}}^{(i)} f}{p + k_{\text{off}}^{(i)}}, \\
c^{(o)} &= \frac{k_{\text{on}}^{(o)} f + c_{\text{eq}}^{(o)}}{p + k_{\text{off}}^{(o)}}, \\
f &= \frac{f_{\text{eq}}(1 - \epsilon^2) \left[1 + \frac{k_{\text{on}}^{(o)}}{p + k_{\text{off}}^{(o)}} \right]}{p \left[1 + \epsilon^2 \frac{k_{\text{on}}^{(i)}}{p + k_{\text{off}}^{(i)}} + (1 - \epsilon^2) \frac{k_{\text{on}}^{(o)}}{p + k_{\text{off}}^{(o)}} \right]}, \tag{29}
\end{aligned}$$

where we used the fact that $k_{\text{off}}^{(o)} c_{\text{eq}}^{(o)} = k_{\text{on}}^{(o)} f_{\text{eq}}$. The total signal is $\mathcal{I}(p) = f + c^{(i)}$, or,

$$\mathcal{I}(p) = \left(1 + \frac{k_{\text{on}}^{(i)}}{p + k_{\text{off}}^{(i)}} \right) \frac{f_{\text{eq}}(1 - \epsilon^2) \left(1 + \frac{k_{\text{on}}^{(o)}}{p + k_{\text{off}}^{(o)}} \right)}{p \left[1 + \epsilon^2 \frac{k_{\text{on}}^{(i)}}{p + k_{\text{off}}^{(i)}} + (1 - \epsilon^2) \frac{k_{\text{on}}^{(o)}}{p + k_{\text{off}}^{(o)}} \right]}. \tag{30}$$

As in Section 1.4, we obtain $\mathcal{I}(t)$ by numerical Laplace inversion $p \rightarrow t$. The long times limit is exactly as in Section 1.5.1.

1.5.3 Diffusion only

The limit when the process is dominated by diffusion is obtained by substituting $k_{\text{on}}^{(i)} = k_{\text{on}}^{(o)} = 0$ in the equations of Section 1.4. We note that when $r_m = r_s \ll r_n$ and $\beta = 0$, the total signal can be approximated by the Soumpasis equation [7]

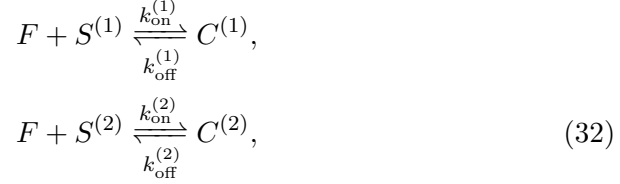
$$\mathcal{I}(t) = e^{-\frac{\tau}{t}} \left[I_0 \left(\frac{\tau}{t} \right) + I_1 \left(\frac{\tau}{t} \right) \right], \tag{31}$$

where $\tau = r_s^2/(2D)$ is the typical recovery time.

1.6 Two binding states

The generalization of our model to multiple binding states is straightforward. We give the definitions and the final equations for the case of two binding states. Denote as before the free particles by F (concentration f), the bound particles of type (1) as $C^{(1)}$ (concentration $c^{(1)}$), and the bound particles of

type (2) as $C^{(2)}$ ($c^{(2)}$). Static particles have constant (in space and time) concentration β . The reactions are:



where

$$\begin{aligned} k_{\text{on}}^{(1)}(r) &= \begin{cases} k_{\text{on}}^{(1,i)} & r < r_s, \\ k_{\text{on}}^{(1,o)} & r_s < r < r_n. \end{cases} \\ k_{\text{off}}^{(1)}(r) &= \begin{cases} k_{\text{off}}^{(1,i)} & r < r_s, \\ k_{\text{off}}^{(1,o)} & r_s < r < r_n, \end{cases} \\ k_{\text{on}}^{(2)}(r) &= \begin{cases} k_{\text{on}}^{(2,i)} & r < r_s, \\ k_{\text{on}}^{(2,o)} & r_s < r < r_n. \end{cases} \\ k_{\text{off}}^{(2)}(r) &= \begin{cases} k_{\text{off}}^{(2,i)} & r < r_s, \\ k_{\text{off}}^{(2,o)} & r_s < r < r_n. \end{cases} \end{aligned} \quad (33)$$

With two binding states, it is possible to implement a biological model in which there are different types of binding sites inside and outside the spot. We assume as in Section 1.1 that the binding sites are immobile and the bleaching does not disturb the chemical equilibrium. We can therefore use the pseudo-on rates as in Section 1.2 and obtain the following reaction-diffusion system:

$$\begin{aligned} \frac{\partial f}{\partial t} &= D\nabla^2 f - k_{\text{on}}^{(1)} f + k_{\text{off}}^{(1)} c^{(1)} - k_{\text{on}}^{(2)} f + k_{\text{off}}^{(2)} c^{(2)}, \\ \frac{\partial c^{(1)}}{\partial t} &= k_{\text{on}}^{(1)} f - k_{\text{off}}^{(1)} c^{(1)}, \\ \frac{\partial c^{(2)}}{\partial t} &= k_{\text{on}}^{(2)} f - k_{\text{off}}^{(2)} c^{(2)}, \\ \beta(t) &= \beta(t=0). \end{aligned} \quad (34)$$

The boundary condition is as in Section 1.2:

$$\left. \frac{\partial}{\partial r} f(r, t) \right|_{r=r_n} = 0. \quad (35)$$

The total signal is the sum of the concentrations of the static particles, the free particles, the bound particles of type (1), and the bound particles of type (2) in the region $r < r_s$. Thus, at $t < 0$ when the system is in equilibrium,

$$\mathcal{I}(t < 0) = f_{\text{eq}} \left(1 + \frac{k_{\text{on}}^{(1,i)}}{k_{\text{off}}^{(1,i)}} + \frac{k_{\text{on}}^{(2,i)}}{k_{\text{off}}^{(2,i)}} \right) + \beta = 1. \quad (36)$$

The initial conditions can therefore be written as:

$$\begin{aligned} f(t=0) &= f_{\text{eq}} = (1 - \beta) \left(1 + \frac{k_{\text{on}}^{(1,i)}}{k_{\text{off}}^{(1,i)}} + \frac{k_{\text{on}}^{(2,i)}}{k_{\text{off}}^{(2,i)}} \right)^{-1}, \\ c^{(1)}(t=0) &= \begin{cases} 0 & r < r_s, \\ c_{\text{eq}}^{(1,o)} = (1 - \beta) \frac{k_{\text{on}}^{(1,o)}}{k_{\text{off}}^{(1,o)}} \left(1 + \frac{k_{\text{on}}^{(1,i)}}{k_{\text{off}}^{(1,i)}} + \frac{k_{\text{on}}^{(2,i)}}{k_{\text{off}}^{(2,i)}} \right)^{-1} & r_s < r < r_n, \end{cases} \\ c^{(2)}(t=0) &= \begin{cases} 0 & r < r_s, \\ c_{\text{eq}}^{(2,o)} = (1 - \beta) \frac{k_{\text{on}}^{(2,o)}}{k_{\text{off}}^{(2,o)}} \left(1 + \frac{k_{\text{on}}^{(1,i)}}{k_{\text{off}}^{(1,i)}} + \frac{k_{\text{on}}^{(2,i)}}{k_{\text{off}}^{(2,i)}} \right)^{-1} & r_s < r < r_n, \end{cases} \\ \beta(t=0) &= \begin{cases} 0 & r < r_s, \\ \beta & r_s < r < r_n. \end{cases} \end{aligned} \quad (37)$$

Laplace transforming Eq. (34) $t \rightarrow p$ as in Section 1.4 we obtain for the bound particles:

$$\begin{aligned} c^{(1)} &= \begin{cases} \frac{k_{\text{on}}^{(1,i)} f}{p + k_{\text{off}}^{(1,i)}} & r < r_s, \\ \frac{c_{\text{eq}}^{(1,o)} + k_{\text{on}}^{(1,o)} f}{p + k_{\text{off}}^{(1,o)}} & r_s < r < r_n, \end{cases} \\ c^{(2)} &= \begin{cases} \frac{k_{\text{on}}^{(2,i)} f}{p + k_{\text{off}}^{(2,i)}} & r < r_s, \\ \frac{c_{\text{eq}}^{(2,o)} + k_{\text{on}}^{(2,o)} f}{p + k_{\text{off}}^{(2,o)}} & r_s < r < r_n. \end{cases} \end{aligned} \quad (38)$$

For the free particles, we obtain the same equation as in Section 1.4

$$\nabla^2 f(r, p) = \begin{cases} q_i^2 f(r, p) & r < r_s, \\ q_o^2 f(r, p) - V & r_s < r < r_n, \end{cases} \quad (39)$$

but where now

$$\begin{aligned} q_i^2 &= \frac{p}{D} \left(1 + \frac{k_{\text{on}}^{(1,i)}}{p + k_{\text{off}}^{(1,i)}} + \frac{k_{\text{on}}^{(2,i)}}{p + k_{\text{off}}^{(2,i)}} \right), \\ q_o^2 &= \frac{p}{D} \left(1 + \frac{k_{\text{on}}^{(1,o)}}{p + k_{\text{off}}^{(1,o)}} + \frac{k_{\text{on}}^{(2,o)}}{p + k_{\text{off}}^{(2,o)}} \right), \end{aligned} \quad (40)$$

and

$$V = \frac{f_{\text{eq}}}{D} \left(1 + \frac{k_{\text{on}}^{(1,o)}}{p + k_{\text{off}}^{(1,o)}} + \frac{k_{\text{on}}^{(2,o)}}{p + k_{\text{off}}^{(2,o)}} \right). \quad (41)$$

The solution of these equations is exactly as in Section 1.4; one simply must use the new definitions of q_i , q_o , and V (e.g., in Eq. (20) for A). The total signal is

$$\mathcal{I}(p) = 2A \left(1 + \frac{k_{\text{on}}^{(1,i)}}{p + k_{\text{off}}^{(1,i)}} + \frac{k_{\text{on}}^{(2,i)}}{p + k_{\text{off}}^{(2,i)}} \right) \frac{I_1(q_i r_m)}{q_i r_m}. \quad (42)$$

For long times,

$$\mathcal{I}(t \rightarrow \infty) = (1 - \beta) \frac{1}{1 + \frac{\epsilon^2}{1 - \epsilon^2} \frac{\rho_i}{\rho_o}}, \quad (43)$$

exactly as in Section 1.5.1, but where now $\rho_i = 1 + \frac{k_{\text{on}}^{(1,i)}}{k_{\text{off}}^{(1,i)}} + \frac{k_{\text{on}}^{(2,i)}}{k_{\text{off}}^{(2,i)}}$ and $\rho_o = 1 + \frac{k_{\text{on}}^{(1,o)}}{k_{\text{off}}^{(1,o)}} + \frac{k_{\text{on}}^{(2,o)}}{k_{\text{off}}^{(2,o)}}$. In the reaction-dominant limit, repeating the calculation of Section 1.5.2 gives

$$\begin{aligned} \mathcal{I}(p) &= \left(1 + \frac{k_{\text{on}}^{(1,i)}}{p + k_{\text{off}}^{(1,i)}} + \frac{k_{\text{on}}^{(2,i)}}{p + k_{\text{off}}^{(2,i)}} \right) \times \\ &\quad f_{\text{eq}}(1 - \epsilon^2) \left(1 + \frac{k_{\text{on}}^{(1,o)}}{p + k_{\text{off}}^{(1,o)}} + \frac{k_{\text{on}}^{(2,o)}}{p + k_{\text{off}}^{(2,o)}} \right) \\ &\quad \times \frac{1}{p \left[1 + \epsilon^2 \left(\frac{k_{\text{on}}^{(1,i)}}{p + k_{\text{off}}^{(1,i)}} + \frac{k_{\text{on}}^{(2,i)}}{p + k_{\text{off}}^{(2,i)}} \right) + (1 - \epsilon^2) \left(\frac{k_{\text{on}}^{(1,o)}}{p + k_{\text{off}}^{(1,o)}} + \frac{k_{\text{on}}^{(2,o)}}{p + k_{\text{off}}^{(2,o)}} \right) \right]}. \end{aligned} \quad (44)$$

2 Processing of experimental data

2.1 The bleaching radius

An important parameter of our model is the bleaching radius. We assumed that the bleaching profile is a perfect circle with radius r_s , that is, all

molecules with $r < r_s$ are completely bleached while all molecules with $r > r_s$ aren't. This is not necessarily true in reality due to (a) the Gaussian profile of the laser beam [8] and (b) diffusion during bleaching that results in partial recovery of the signal before the end of the bleaching stage of the experiment [9].

Directly including these factors in our biological model is not always mathematically feasible (some approaches are presented in, e.g., [9, 10, 11, 12, 13, 14, 15], for conditions somewhat different than ours). In particular, it is likely to be extremely hard to incorporate both inhomogeneous binding and non-circular profile (McNally PC). To avoid such complications but still take into account the effects on a non-circular bleaching profile, we adopted the method used, e.g., in [8, 16, 4, 17]. In this method, a circular bleaching profile is assumed, but the bleaching radius is not the software-preset radius but is instead an *effective* radius determined from the *observed* non-uniform bleaching profile.

To obtain the effective radius, we captured X post-bleach images (were cells immobilized? they shouldn't be to account for diffusion during bleaching). We then calculated, for each figure, the average intensity $\langle \mathcal{I}(r) \rangle$, where r is the distance from the bleaching spot center, and the average is over all images. We let $r_M = \arg \max_r \langle \mathcal{I}(r) \rangle$ and $\langle \mathcal{I}'(r) \rangle \equiv \langle \mathcal{I}(r) \rangle / \langle \mathcal{I}(r_M) \rangle$, such that $\langle \mathcal{I}'(r_M) \rangle = 1$ (alternatively, we defined $\langle \mathcal{I}(r_M) \rangle$ as the average intensity for all points with $r > X$, and pruned to 1 each value of $\langle \mathcal{I}'(r) \rangle$ larger than 1). We then defined the average *bleaching intensity* $\langle B(r) \rangle \equiv 1 - \langle \mathcal{I}'(r) \rangle$. Finally, we computed the average *total bleached area* $\langle S \rangle = \int_0^{r_M} 2\pi r \langle B(r) \rangle dr$, where the integral was evaluated using the trapezoid method. Had the bleaching profile been perfectly circular with radius r_s , we would have had $\langle S \rangle = \pi r_s^2$. Equating these two expressions for the average bleached area we obtain

$$r_s = \sqrt{\int_0^{r_M} 2r \langle B(r) \rangle dr}. \quad (45)$$

Thus, the effective radius is that of a perfectly circular bleaching profile that would yield that same amount of bleaching as the experimental one.

We also considered calculating the bleaching intensity $\langle B(r) \rangle$ directly, by subtracting the post-bleach image from the pre-bleach image. We corrected for global intensity changes by subtracting a constant value from the resulting $\langle B(r) \rangle$ such that the average of $\langle B(r) \rangle$ for $r > X$ will be zero.

2.2 The nuclear radius

The radius of the nucleus r_n was obtained by calculating first the average (over Z images) of the area of the nucleus $\langle S_n \rangle$. The radius was then obtained from $\pi r_n^2 = \langle S_n \rangle$.

2.3 The monitoring radius

The monitoring radius was set to...

2.4 Data acquisition and normalization

Captured images were processed first by background subtraction (how?). The rate of fluorescence loss during observation was measured in a neighboring cell and used to normalize the signal intensity at the investigated cell. (details?). The normalized signal was then divided by the average (how?) pre-bleach signal. The final normalized intensity therefore satisfies $\mathcal{I}(t=0) = 1$; $0 \leq \mathcal{I}(t) \leq 1$. For each cell line or treatment, recovery curves from Y different cells were averaged. The obtained time series was then logarithmically binned, i.e., data points were averaged over time periods of exponentially increasing length. The averaged curve $\mathcal{I}_{\text{exp}}(t)$ was fit to the model (Section 1.2) to infer the kinetic parameters, as described in the next subsection.

2.5 The static fraction

The concentration of the static particles, β , was obtained as follows. We performed a FRAP experiment with a particularly small r_s , such that $\epsilon = r_s/r_n \rightarrow 0$. In this case, $\mathcal{I}(t \rightarrow \infty) = (1 - \beta)$ (Eq. (26)), enabling direct measurement of β .

(Add details)

2.6 Data fitting

The first step in data fitting was the determination of the kinetic model, as follows.

- One reaction and diffusion. In that case, the parameters to be fit are $D, k_{\text{on}}, k_{\text{off}}$. We use Eq. (22) for the total signal $\mathcal{I}(t)$.
- Diffusion only (no reactions). In that case we set $k_{\text{on}} = 0$ and the only parameter to be fit is D . Here we also Eq. (22).

- Two reactions and diffusion. Here the parameters to be fit are $D, k_{\text{on}}^{(1)}, k_{\text{off}}^{(1)}, k_{\text{on}}^{(2)}, k_{\text{off}}^{(2)}$ and we use Eq. (42).
- One state reaction-dominant. In that case, diffusion is assumed to be infinitely fast and we only fit $k_{\text{on}}, k_{\text{off}}$. We use Eq. (30) for the total signal.
- Two states reaction-dominant. Here we fit $k_{\text{on}}^{(1)}, k_{\text{off}}^{(1)}, k_{\text{on}}^{(2)}, k_{\text{off}}^{(2)}$. We use Eq. (44).
- For each reaction, the values of $k_{\text{on}}^{(i)}, k_{\text{off}}^{(i)}, k_{\text{on}}^{(o)}, k_{\text{off}}^{(o)}$ are determined based on the binding model:
 - Homogeneous binding. In that case, $k_{\text{on}}^{(i)} = k_{\text{on}}^{(o)} = k_{\text{on}}, k_{\text{off}}^{(i)} = k_{\text{off}}^{(o)} = k_{\text{off}}$.
 - Internal binding. In that case, $k_{\text{on}}^{(i)} = k_{\text{on}}, k_{\text{on}}^{(o)} = 0, k_{\text{off}}^{(i)} = k_{\text{off}}, k_{\text{off}}^{(o)}$ irrelevant.
 - External binding. In that case, $k_{\text{on}}^{(o)} = k_{\text{on}}, k_{\text{on}}^{(i)} = 0, k_{\text{off}}^{(o)} = k_{\text{off}}, k_{\text{off}}^{(i)}$ irrelevant.

The experimental parameters r_s, r_n, r_m , and β are determined as explained in Sections 2.1, 2.2, 2.3, and 2.5, respectively. At this point, we have an equation for the total signal $\mathcal{I}(t)$ that depends only on parameters that we either obtained experimentally or we are about to fit.

Initial guess for the parameters (any subset of $D, k_{\text{on}}^{(1)}, k_{\text{off}}^{(1)}, k_{\text{on}}^{(2)}, k_{\text{off}}^{(2)}$) was taken from the literature or obtained from manual coarse-grained scanning of the parameter space. A time vector was created that contains the experimental time points. The Matlab [18] routine *lsqcurvefit* was used to fit the model to the experimental curve, starting from the initial guess. All fitted parameters were forced to be positive. The standard error of the fitted parameters were calculated with the Matlab function *nlparci* (by forcing the function to return the *se* variable instead of the confidence intervals). The inverse Laplace transforms were computed with the *invlap.m* Matlab function [19]. The maximum theoretical recovery was calculated from Eq. (26) for one reaction and from Eq. (43) for two reactions.

2.7 Testing the quality of the fit

The first measure of the quality of the fit was the standard error (SE) in the values of the fitted parameters (as calculated by Matlab, see Section 2.6).

We give the following goodness of fit index. We first calculate the percentage of the SE from the parameter value (coefficient of variation like). We then report the maximal percentage across all fitted parameters. The smallest this measure is, the better the fit.

The averaged squared error between the model total signal and the experimental recovery curve (Mean SSE) = $\frac{1}{t_m} \sum_{i=0}^{t_m} [\mathcal{I}(t_i) - \mathcal{I}_{\text{exp}}(t_i)]^2$ ((t_0, t_1, \dots, t_m) is the time vector) is a measure of the deviation between of the model and the experiment. To test the quality of the fit, we plotted the Mean SSE for several values of the fitted parameters, centered around the values suggested by the fitting procedure. Specifically, values of D , k_{on} and k_{off} were generated in equal spacing (on a logarithmic scale), and $\mathcal{I}(t)$ was calculated based on the kinetic model for each parameter combination. We then plotted the SSE vs. D and vs. k_{on} and k_{off} . In the latter case, we plotted a two-dimensional array, color-coded according to the Mean SSE, producing the quality-of-fit ‘heat map’. A distinguishable minimum in the Mean SSE plot at the values returned by the fitting procedure indicates a good fit.

Even for a deep minimum, it could be that starting the fitting process from a different initial guess would end up in a different minimum which has an even lower Mean SSE. We therefore repeated the fitting procedure from a sample of random starting points. We started with the parameter values that were obtained from the user-supplied initial guess. For reaction rate parameters (k_{ons} and k_{offs}), we multiplied the parameter with 10^u , where u is uniformly distributed in $[-X, X]$. For the other parameters, we randomly either multiplied or divided by u , where u is uniformly distributed in $[1, Y]$. This way we scan a large range of order of magnitudes of reaction rates, since they can vary widely, but remain within the same order of magnitude for the other parameters.

After drawing the random initial guesses, we ran the fitting procedure starting from these guesses and recorded the fitted parameters and the Mean SSEs. To quantify the difference in the fitting parameters, we calculated, for each random initial guess, the percentage by which each fitted parameter value differs from the value fitted with the user-supplied initial guess. We then calculated the maximum of those percentages over all parameters (e.g., D , k_{on} , k_{off} , etc.), giving a single index of disparity for each random initial guess. We then plotted the Mean SSE vs. this index. If the fit was unique, there will be two clusters of points: (1) points where the fitted parameters are not too different from the user-supplied fitted values (the fitting procedure converged to the same minimum), and the Mean SSE is similar; (2) points where the fitted parameters are very different from the user-supplied fitted values, and the Mean SSE is much larger than the user-supplied one.

This means that other minima in the SSE landscape are much shallower than the user-supplied one. On the other hand, if there are points where the parameter values are different from the user-supplied fitted values but the Mean SSE is equal or smaller than the user-supplied one, this means that the minimum originally found is not reliable. As a quantitative measure, we report the number of random starting points that yielded smaller Mean SSE than the user-supplied one, and the ratio between the median Mean SSEs of random starting points whose fitted parameters are far from the user-supplied fitted parameters (by at least $X\%$) to the user-supplied Mean SSE. The latter measure can roughly quantify the increase in the Mean SSE when the fitting procedure reached a different minimum from the one originally found.

2.8 Simultaneous fitting of multiple experiments

Fitting means finding the parameter set that will minimize the SSE. We attempt to fit up to five parameters; such a multi-dimensional optimization problem is very hard—it is almost impossible to perform an exhaustive search that will find the absolute, global minimum. Fitting procedures thus usually search a good local minimum. The specific minimum we end at depends on the structure of the SSE space. We observed in heat maps of real experiments that the SSE space is in many cases quite flat; the global minimum can be easily missed.

We therefore fitted multiple experiments *in parallel*. The parameter set to fit was determined as in Section 2.6. For each set of values taken by the fitted parameters, we generated a model curve for each experiment separately. If experiments had different experimental configurations, e.g., different bleaching or monitoring radii, this was taken into account when solving the model. We then *concatenated* all the experimental curves into one long time series, and did similarly for the model curves. We searched for parameters that fit the *combined* experimental data. This way, we increased significantly the number of data points we fit our data to, and hopefully reached a deeper minimum. A similar approach was proposed in [15, 20], where multiple FRAP curves were simultaneously fitted.

3 A FLIP model

To our knowledge, the FLIP model described below, although based on the framework of [1], is the first quantitative theory of FLIP.

3.1 Model definition

In FLIP, the region $r < r_s$ is continuously bleached and the fluorescence loss in $r > r_s$ is observed. We use the same basic reaction-diffusion model as in Section 1, and consider first the single binding state reaction $F + S \xrightleftharpoons[k_{\text{off}}]{k_{\text{on}}} C$.

The reaction-diffusion equations remain the same,

$$\begin{aligned}\frac{\partial f}{\partial t} &= D\nabla^2 f - k_{\text{on}}f + k_{\text{off}}c, \\ \frac{\partial c}{\partial t} &= k_{\text{on}}f - k_{\text{off}}c, \\ \beta &= \beta(t = 0).\end{aligned}\tag{46}$$

These equations, as well as the reaction rates k_{on} and k_{off} , are defined only for $r_s < r < r_n$, and therefore the reaction rates need not be split to the different regions as in Section 1.2. One boundary condition is the reflecting walls of the nucleus:

$$\left. \frac{\partial}{\partial r} f(r, t) \right|_{r=r_n} = 0.\tag{47}$$

The other boundary condition describes the continuous bleaching of the spot $r < r_s$. If the bleaching is perfectly continuous for all times $t > 0$, the bleaching boundary condition is given by

$$f(r = r_s, t) = 0.\tag{48}$$

This is an absorbing boundary at $r = r_s$, since any molecule that arrives to $r < r_s$ loses its visibility and therefore disappears. In practice, due to experimental obstacles (details?), the spot $r < r_s$ is not continuously bleached, and some of the molecules that arrive into the spot are able to escape without losing their fluorescence. We denote the times the spot is bleached as the bleaching periods.

To account for the discontinuous nature of the bleaching, we approximate the boundary at $r = r_s$ as an imperfectly absorbing boundary (or radiation boundary [5]). In this boundary, particles are either absorbed or reflected when they hit the boundary. This is an approximation, because particles in FLIP are not reflected immediately when they hit the boundary, but can rather travel in the spot. If a particle is still in the spot at the time of the next bleaching period, it will then be eliminated. Otherwise, the particle will be outside the spot at the next bleaching period and will thus survive. The latter case can be approximated as if the particle has been reflected already when it first hit the spot boundary.

Formally, the imperfect absorption boundary condition is

$$f(r = r_s, t) = \alpha \left. \frac{\partial}{\partial r} f(r, t) \right|_{r=r_s}, \quad (49)$$

where α has units of 1/length. Eq. (48) is obtained from (49) in the limit $\alpha \rightarrow 0$ ($\alpha \rightarrow \infty$ is the perfect reflection limit).

In FLIP, the total signal $\mathcal{I}(t)$ is defined as the average concentration of visible molecules in the ring limited by the circles $r = r_1$ and $r = r_2$, $r_s < r_1 < r_2 < r_n$. Here, there are two monitoring radii, r_1 and r_2 . Mathematically,

$$\mathcal{I}(t) = \frac{1}{\pi(r_2^2 - r_1^2)} \int_{r_1}^{r_2} 2\pi r [f(r, t) + c(r, t) + \beta(r, t)] dr. \quad (50)$$

To obtain the initial conditions (again, only for $r_s < r < r_n$) we assume the system is in equilibrium prior to the beginning of the experiment. The equilibrium concentrations f_{eq} and c_{eq} are determined by the equilibrium equation $k_{\text{on}}f_{\text{eq}} = k_{\text{off}}c_{\text{eq}}$ and by the normalization of the total signal $f_{\text{eq}} + c_{\text{eq}} + \beta = 1$ (as before, $\beta(r, t) = \beta(r, t = 0) = \beta$ is the concentration of the static particles). Thus

$$\begin{aligned} f(r, t = 0) &= f_{\text{eq}} = (1 - \beta) \frac{k_{\text{off}}}{k_{\text{on}} + k_{\text{off}}}, \\ c(r, t = 0) &= c_{\text{eq}} = (1 - \beta) \frac{k_{\text{on}}}{k_{\text{on}} + k_{\text{off}}}. \end{aligned} \quad (51)$$

By that we completely specified our FLIP model.

3.2 Model solution

We approach the FLIP model as in Section 1.4. Laplace transforming Eq. (46) we obtain

$$\begin{aligned} pf - f_{\text{eq}} &= D\nabla^2 f - k_{\text{on}}f + k_{\text{off}}c, \\ pc - c_{\text{eq}} &= k_{\text{on}}f - k_{\text{off}}c. \end{aligned} \quad (52)$$

The solution of c in terms of f is

$$c = \frac{c_{\text{eq}} + k_{\text{on}}f}{p + k_{\text{off}}}. \quad (53)$$

Substituting Eq. (53) in Eq. (52) we have

$$\nabla^2 f = q^2 f - V, \quad (54)$$

where $q^2 = \frac{p}{D} \left(1 + \frac{k_{\text{on}}}{p+k_{\text{off}}}\right)$ and $V = \frac{f_{\text{eq}}}{D} \left(1 + \frac{k_{\text{on}}}{p+k_{\text{off}}}\right)$ (we used $k_{\text{off}}c_{\text{eq}} = k_{\text{on}}f_{\text{eq}}$). This is the same as in Section 1.4. The solution for f is

$$f = AI_0(qr) + BK_0(qr) + \frac{V}{q^2}. \quad (55)$$

Applying the boundary conditions (47) and (49) gives equations for the prefactors A and B :

$$\begin{aligned} AqI_1(qr_n) - BqK_1(qr_n) &= 0, \\ AI_0(qr_s) + BK_0(qr_s) + \frac{V}{q^2} &= \alpha [AqI_1(qr_s) - BqK_1(qr_s)]. \end{aligned} \quad (56)$$

This yields

$$\begin{aligned} A &= \frac{V K_1(qr_n)}{q^2 \text{den}}, \\ B &= \frac{V I_1(qr_n)}{q^2 \text{den}}, \end{aligned} \quad (57)$$

where

$$\text{den} = \alpha q I_1(qr_s) K_1(qr_n) - \alpha q I_1(qr_n) K_1(qr_s) - I_0(qr_s) K_1(qr_n) - I_1(qr_n) K_0(qr_s). \quad (58)$$

The total signal is given by

$$\begin{aligned} \mathcal{I}(p) &= \frac{1}{\pi (r_2^2 - r_1^2)} \int_{r_1}^{r_2} 2\pi r [f(r, p) + c(r, p) + \beta(r, p)] dr \\ &= \frac{1}{\pi (r_2^2 - r_1^2)} \int_{r_1}^{r_2} 2\pi r \left[f(r, p) \left(1 + \frac{k_{\text{on}}}{p+k_{\text{off}}}\right) + \frac{c_{\text{eq}}}{p+k_{\text{off}}} + \frac{\beta}{p} \right] dr \\ &= \frac{\beta}{p} + \frac{c_{\text{eq}}}{p+k_{\text{off}}} + \frac{1 + \frac{k_{\text{on}}}{p+k_{\text{off}}}}{\pi (r_2^2 - r_1^2)} \int_{r_1}^{r_2} 2\pi r f(r, t) dr \\ &= \frac{\beta}{p} + \frac{c_{\text{eq}}}{p+k_{\text{off}}} + \frac{1 + \frac{k_{\text{on}}}{p+k_{\text{off}}}}{\pi (r_2^2 - r_1^2)} \int_{r_1}^{r_2} 2\pi r \left[AI_0(qr) + BK_0(qr) + \frac{V}{q^2} \right] dr \\ &= \frac{\beta}{p} + \frac{c_{\text{eq}}}{p+k_{\text{off}}} + \left(1 + \frac{k_{\text{on}}}{p+k_{\text{off}}}\right) \times \\ &\quad \times \left[\frac{V}{q^2} + 2A \frac{r_2 I_1(qr_2) - r_1 I_1(qr_1)}{q (r_2^2 - r_1^2)} - 2B \frac{r_2 K_1(qr_2) - r_1 K_1(qr_1)}{q (r_2^2 - r_1^2)} \right], \end{aligned} \quad (59)$$

where we used the relations $[rI_1(r)]' = rI_0(r)$, $[rK_1(r)]' = -rK_0(r)$, and $\mathcal{L}\{\beta\} = \beta/p$. Thus, for given $\beta, r_s, r_n, D, k_{\text{on}}, k_{\text{off}}, \alpha, r_1, r_2$, the total signal $\mathcal{I}(t)$ can be obtained from Eq. (59) upon Laplace inversion $p \rightarrow t$. This is done numerically, as explained in Section 3.4.

3.3 Special cases

In this Section we briefly treat a number of special cases, as in Section 1.5.

3.3.1 Infinite times

In FLIP, free visible molecules are continuously lost in the bleached spot. Also, every bound molecule eventually detaches from the binding site and becomes free (after which it is bleached). Thus, after long enough times, the total observed signal decays to the fraction of static particle β .

3.3.2 The reaction-dominant limit

The reaction-dominant limit is much simpler compared to FRAP (Section 1.5.2). Since the diffusion of the free molecules is extremely fast, it can be assumed that all molecules are bleached immediately once they become free. Thus, $f = 0$ at all times ($t > 0$). We are left with an ordinary differential equation for c ,

$$\frac{\partial c}{\partial t} = -k_{\text{off}}c, \quad (60)$$

with the initial condition $c(t = 0) = c_{\text{eq}}$. The solution (and thereby the total signal) is:

$$\mathcal{I}(t) = \beta + c(t) = \beta + c_{\text{eq}}e^{-k_{\text{off}}t}. \quad (61)$$

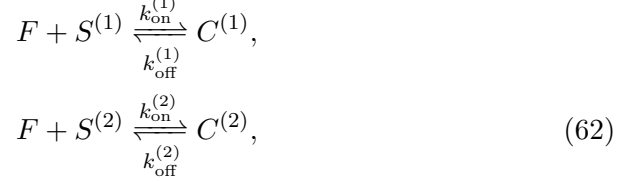
3.3.3 Diffusion only

The limit when the process is dominated by diffusion is obtained simply by setting $k_{\text{on}} = 0$, as in FRAP (Section 1.5.3).

3.3.4 Two binding states

In FLIP, adding another binding state does not fundamentally change the physical situation, since in FLIP we only probe the region outside the spot. Two binding states can be interesting though if we measure the fluorescent signal only from one species of bound particles. According to the model, the binding sites of both types are evenly spread in the nucleus, prohibiting measurement of one species only. However, it is sometimes experimentally possible (e.g., based on external information such as the physical appearance of the bound particles of each species) to single out the fluorescence coming from one type of sites. We state here the final results for this case. The

reactions are (Section 1.6)



where here the reaction rates are defined only in the region $r_s < r < r_n$. The reaction-diffusion system of equations is:

$$\begin{aligned}
\frac{\partial f}{\partial t} &= D\nabla^2 f - k_{\text{on}}^{(1)} f + k_{\text{off}}^{(1)} c^{(1)} - k_{\text{on}}^{(2)} f + k_{\text{off}}^{(2)} c^{(2)}, \\
\frac{\partial c^{(1)}}{\partial t} &= k_{\text{on}}^{(1)} f - k_{\text{off}}^{(1)} c^{(1)}, \\
\frac{\partial c^{(2)}}{\partial t} &= k_{\text{on}}^{(2)} f - k_{\text{off}}^{(2)} c^{(2)}, \\
\beta &= \beta(t=0).
\end{aligned} \tag{63}$$

The boundary condition for f is as in Section 3.1. The total measured signal is:

$$\mathcal{I}(t) = \frac{1}{\pi(r_2^2 - r_1^2)} \int_{r_1}^{r_2} 2\pi r \left[f(r, t) + c^{(1)}(r, t) + \beta(r, t) \right] dr, \tag{64}$$

namely we measure the fluorescence coming from static particles, free particles and bound particles only of type (1). Assuming equilibrium for $t < 0$ and normalization of $\mathcal{I}(t)$, the initial conditions are

$$\begin{aligned}
f(r, t=0) &= f_{\text{eq}} = (1 - \beta) \frac{k_{\text{off}}^{(1)}}{k_{\text{on}}^{(1)} + k_{\text{off}}^{(1)}}, \\
c^{(1)}(r, t=0) &= c_{\text{eq}}^{(1)} = (1 - \beta) \frac{k_{\text{on}}^{(1)}}{k_{\text{on}}^{(1)} + k_{\text{off}}^{(1)}}, \\
c^{(2)}(r, t=0) &= c_{\text{eq}}^{(2)} = (1 - \beta) \frac{k_{\text{on}}^{(2)}}{k_{\text{off}}^{(2)}} \frac{k_{\text{off}}^{(1)}}{k_{\text{on}}^{(1)} + k_{\text{off}}^{(1)}}.
\end{aligned} \tag{65}$$

In Laplace space $t \rightarrow p$, the concentrations of the bound particles are

$$\begin{aligned}
c^{(1)} &= \frac{c_{\text{eq}}^{(1)} + k_{\text{on}}^{(1)} f}{p + k_{\text{off}}^{(1)}}, \\
c^{(2)} &= \frac{c_{\text{eq}}^{(2)} + k_{\text{on}}^{(2)} f}{p + k_{\text{off}}^{(2)}}.
\end{aligned} \tag{66}$$

For the free particles, Eq. (63) reduces to

$$\nabla^2 f = q^2 f - V, \quad (67)$$

where

$$\begin{aligned} q^2 &= \frac{p}{D} \left(1 + \frac{k_{\text{on}}^{(1)}}{p + k_{\text{off}}^{(1)}} + \frac{k_{\text{on}}^{(2)}}{p + k_{\text{off}}^{(2)}} \right), \\ V &= \frac{f_{\text{eq}}}{D} \left(1 + \frac{k_{\text{on}}^{(1)}}{p + k_{\text{off}}^{(1)}} + \frac{k_{\text{on}}^{(2)}}{p + k_{\text{off}}^{(2)}} \right). \end{aligned} \quad (68)$$

The solution of f , $c^{(1)}$, and $c^{(2)}$ is exactly as in Section 3.2, but the new definitions of q^2 and V must be used. Substituting f and $c^{(1)}$ in Eq. (64) for the total signal,

$$\begin{aligned} \mathcal{I}(p) &= \frac{\beta}{p} + \frac{c_{\text{eq}}^{(1)}}{p + k_{\text{off}}^{(1)}} + \left(1 + \frac{k_{\text{on}}^{(1)}}{p + k_{\text{off}}^{(1)}} \right) \times \\ &\times \left[\frac{V}{q^2} + 2A \frac{r_2 I_1(qr_2) - r_1 I_1(qr_1)}{q(r_2^2 - r_1^2)} - 2B \frac{r_2 K_1(qr_2) - r_1 K_1(qr_1)}{q(r_2^2 - r_1^2)} \right]. \end{aligned} \quad (69)$$

Note that (69) is exactly as (59) (the single binding state) except that k_{on} and k_{off} are replaced by $k_{\text{on}}^{(1)}$ and $k_{\text{off}}^{(1)}$, respectively. This is because when solving for the total signal, we take into account only binding sites of type (1). The infinite time limit, the reaction-dominant limit, and the diffusion only case are exactly as in the case of a single binding state (Sections 3.3.1, 3.3.2, and 3.3.3, respectively).

In case we measure the total fluorescence coming from all visible molecules, the initial conditions become (cf. Eq. (37)):

$$\begin{aligned} f(t=0) &= f_{\text{eq}} = (1 - \beta) \left(1 + \frac{k_{\text{on}}^{(1)}}{k_{\text{off}}^{(1)}} + \frac{k_{\text{on}}^{(2)}}{k_{\text{off}}^{(2)}} \right)^{-1}, \\ c^{(1)}(t=0) &= c_{\text{eq}}^{(1)} = (1 - \beta) \frac{k_{\text{on}}^{(1)}}{k_{\text{off}}^{(1)}} \left(1 + \frac{k_{\text{on}}^{(1)}}{k_{\text{off}}^{(1)}} + \frac{k_{\text{on}}^{(2)}}{k_{\text{off}}^{(2)}} \right)^{-1}, \\ c^{(2)}(t=0) &= c_{\text{eq}}^{(2)} = (1 - \beta) \frac{k_{\text{on}}^{(2)}}{k_{\text{off}}^{(2)}} \left(1 + \frac{k_{\text{on}}^{(1)}}{k_{\text{off}}^{(1)}} + \frac{k_{\text{on}}^{(2)}}{k_{\text{off}}^{(2)}} \right)^{-1}. \end{aligned} \quad (70)$$

The constants V and q^2 remain the same. The total signal is the average concentration of $f + c^{(1)} + c^{(2)}$ in the ring:

$$\mathcal{I}(p) = \frac{\beta}{p} + \frac{c_{\text{eq}}^{(1)}}{p + k_{\text{off}}^{(1)}} + \frac{c_{\text{eq}}^{(2)}}{p + k_{\text{off}}^{(2)}} + \left(1 + \frac{k_{\text{on}}^{(1)}}{p + k_{\text{off}}^{(1)}} + \frac{k_{\text{on}}^{(2)}}{p + k_{\text{off}}^{(2)}} \right) \times \quad (71)$$

$$\times \left[\frac{V}{q^2} + 2A \frac{r_2 I_1(qr_2) - r_1 I_1(qr_1)}{q(r_2^2 - r_1^2)} - 2B \frac{r_2 K_1(qr_2) - r_1 K_1(qr_1)}{q(r_2^2 - r_1^2)} \right].$$

The reaction dominant limit becomes a double exponential,

$$\mathcal{I}(t) = \beta + c_{\text{eq}}^{(1)} e^{-k_{\text{off}}^{(1)} t} + c_{\text{eq}}^{(2)} e^{-k_{\text{off}}^{(2)} t}. \quad (72)$$

3.4 Data processing

The computational pipeline for data processing is similar to that of FRAP (Section 2). The radii r_s and r_n are obtained as in Sections 2.1 and 2.2, respectively. The static fraction β is equal to the long time limit of the total signal (in any configuration), and thus can be easily estimated. Images are acquired, corrected, and averaged as in Section 2.4. Here, $\mathcal{I}_{\text{exp}}(t)$ is calculated as the average signal intensity in the ring limited by the given parameters r_1 and r_2 . If there are two binding states, we compute the average either over the entire ring or only over these areas in the ring in which we observe bound particles of one species.

The parameters to fit are as follows. For one reaction and diffusion, we fit α , D , k_{on} , and k_{off} (Eq. (59) for the total signal) (or do we always have perfect absorption $\alpha = 0$?). For diffusion only, we fit only α and D (Eq. (59) with $k_{\text{on}} = 0$). For a reaction-dominant process (one reaction, or two reactions when we measure the fluorescence of one species only), we fit k_{on} and k_{off} (Eq. (61); note that c_{eq} depends on k_{on}). With two reactions and diffusion, we fit α , D , $k_{\text{on}}^{(1)}$, $k_{\text{off}}^{(1)}$, $k_{\text{on}}^{(2)}$, or $k_{\text{off}}^{(2)}$ (Eq. (69) if we measure one species and Eq. (71) if we measure both). In a reaction-dominant process with two binding states when we measure both species, we fit $k_{\text{on}}^{(1)}$, $k_{\text{off}}^{(1)}$, $k_{\text{on}}^{(2)}$, and $k_{\text{off}}^{(2)}$ (Eq. (72)).

For each experimental data $\mathcal{I}_{\text{exp}}(t)$, we search for the parameters that give the best fit of $\mathcal{I}(t)$ to $\mathcal{I}_{\text{exp}}(t)$. We create an initial guess according to the literature, to manual scanning, or to the FRAP results. We then use the Matlab procedures *lsqcurvefit* to calculate the best fit parameters, *nlparci* to calculate confidence intervals, and *invlap* [19] to calculate inverse Laplace transforms, exactly as in Section 2.6. Plots of the sum of squared errors (between $\mathcal{I}_{\text{exp}}(t)$ and $\mathcal{I}(t)$) vs. D or vs. k_{on} and k_{off} are generated as in Section

2.6. We also combine FLIP curves and FRAP curves for simultaneous fit (as long as the binding model and the set of fitted parameters are the same) as in Section 2.8.

3.5 Comment

Theory was developed for a somewhat different continuous photobleaching experiment [21]. In that paper, a circle was continuously bleached as in FLIP, however in low laser intensity. This causes partial, slow bleaching of the molecules in the spot. The intensity is then averaged over the spot (as opposed to over a ring outside the spot in FLIP).

References

- [1] Brian L. Sprague, Robert L. Pego, Diana A. Stavreva, and James G. McNally. Analysis of binding reactions by fluorescence recovery after photobleaching. *Biophysical Journal*, 86:3473–3495, 2004.
- [2] Brian L. Sprague, Florian Müller, Robert L. Pego, Peter M. Bungay, Diana A. Stavreva, and James G. McNally. Analysis of binding at a single spatially localized cluster of binding sites by fluorescence recovery after photobleaching. *Biophysical Journal*, 91:1169–1191, 2006.
- [3] Mark A. Hallen and Anita T. Layton. Expanding the scope of quantitative FRAP analysis. *Journal of Theoretical Biology*, 262:295–305, 2010.
- [4] Juliane Mai, Saskia Trump, Rizwan Ali, R. Louis Schiltz, Gordon Hager, Thomas Hanke, Irina Lehmann, and Sabine Attinger. Are assumptions about the model type necessary in reaction-diffusion modeling? a FRAP application. *Biophysical Journal*, 100:1178–1188, 2011.
- [5] S. Redner. *A Guide to First-Passage Processes*. Cambridge University Press, 2001.
- [6] Milton Abramowitz and Irene A. Stegun. *Handbook of Mathematical Functions*. Dover Publications, 1964.
- [7] D. M. Soumpasis. Theoretical analysis of fluorescence photobleaching recovery experiments. *Biophysical Journal*, 41:95–97, 1983.

- [8] Florian Mueller, Paul Wach, and James G. McNally. Evidence for a common mode of transcription factor interaction with chromatin as revealed by improved quantitative fluorescence recovery after photobleaching. *Biophysical Journal*, 94:3323–3339, 2008.
- [9] José Braga, Joana M. P. Desterro, and Maria Carmo-Fonseca. Intracellular macromolecular mobility measured by fluorescence recovery after photobleaching with confocal laser scanning microscope. *Molecular Biology of the Cell*, 15:4749–4760, 2004.
- [10] Minchul Kang and Anne K. Kenworthy. A closed-form analytic expression for FRAP formula for the binding diffusion model. *Biophysical Journal*, 95:L13–L15, 2008.
- [11] Minchul Kang, Charles A. Day, Kimberly Drake, Anne K. Kenworthy, and Emmanuele DiBenedetto. A generalization of theory for two-dimensional fluorescence recovery after photobleaching applicable to confocal laser scanning microscopes. *Biophysical Journal*, 97:1501–1511, 2009.
- [12] Minchul Kang, Charles A. Day, Emmanuele DiBenedetto, and Anne K. Kenworthy. A quantitative approach to analyze binding diffusion kinetics by confocal frap. *Biophysical Journal*, 99:2737–2747, 2010.
- [13] Onyinyechi N. Irrechukwu and Marc E. Levenston. Improved estimation of solute diffusivity through numerical analysis of FRAP experiments. *Cellular and Molecular Bioengineering*, 2:104–117, 2009.
- [14] Kouroush Sadegh Zadeh and Hubert J. Montas. A class of exact solutions for biomacromolecule diffusion-reaction in live cells. *Journal of Theoretical Biology*, 264:914–933, 2010.
- [15] Nick Smisdom, Kevin Braeckmans, Hendrik Deschout, Martin vandeVen, Jean-Michel Rigo, Stefaan C. De Smedt, and Marcel Ameloot. Fluorescence recovery after photobleaching on the confocal laser-scanning microscope: generalized model without restriction on the size of the photobleached disk. *Journal of Biomedical Optics*, 16:046021, 2011.
- [16] Holly A. Leddy and Farshid Guilak. Site-specific molecular diffusion in articular cartilage measured using fluorescence recovery after photobleaching. *Annals of Biomedical Engineering*, 31:753–760, 2003.

- [17] Peter Hinow, Carl E. Rogers, Christopher E. Barbieri, Jennifer A. Pietenpol, Anne K. Kenworthy, and Emmanuele DiBenedetto. The dna binding activity of p53 displays reaction-diffusion kinetics. *Biophysical Journal*, 91:330–342, 2006.
- [18] www.mathworks.com.
- [19] K. J. Hollenbeck. INVLAP.M: A matlab function for numerical inversion of Laplace transforms by the de Hoog algorithm. 1998. <http://www.isva.dtu.dk/staff/karl/invlap.htm>.
- [20] Astrid Tannert, Sebastian Tannert, Steffen Burgold, and Michael Schaefer. Convolution-based one and two component FRAP analysis: theory and application. *Eur. Biophys. J.*, 38:649–661, 2009.
- [21] Malte Wachsmuth, Thomas Weidemann, Gabriele Müller, Urs W. Hoffmann-Rohrer, Tobias A. Knoch, Waldemar Waldeck, and Jörg Langowski. Analyzing intracellular binding and diffusion with continuous fluorescence photobleaching. *Biophysical Journal*, 84:3353–3363, 2003.